# Structural and textural study of electrodeposited zinc from alkaline non-cyanide electrolyte

M. S. Chandrasekar · Shanmugasigamani Srinivasan · Malathy Pushpavanam

**Abstract** Pulse electrodeposition was used to produce zinc deposits from an alkaline non-cyanide electrolyte with additives. The influence of additives' concentration and pulse parameters, such as ON-time, OFF-time, and pulse peak current density on the grain size, surface morphology, and crystal orientation were investigated. In an additive-free electrolyte, increase in OFF-time at constant ON-time and peak current density decreases the grain size while the latter increases with increasing ON-time at constant OFF-time and peak current density. A progressive decrease of grain size was observed with increasing peak current density up to 5 $Adm^{-2}$ at constant ON-time and OFF-time in both additive-free electrolyte and bath containing additives. Zinc with an average crystallite size of 34 nm was obtained at 5 $Adm^{-2}$ from electrolyte containing additives. The preferred orientation of the zinc deposits obtained at 6 ms (ON-time), 51.5 ms (OFF-time) and 5 $Adm^{-2}$ (peak current density) with electrolyte containing additives was prismatic [10.0] plane.

## Introduction

Zinc is the most widely used metal for steel protection against corrosion due to its sacrificial nature, low cost, and ease of application [1]. Of the various methods to produce zinc coating, electroplating has a major contribution. The conventionally adopted cyanide formulations are becoming obsolete due to the increasing environmental awareness and more of non-cyanide formulations are being practiced commercially. The alkaline zinc plating baths have several advantages over the acid baths [2–6].

Initially, a cyanide-free alkaline bath was able to give only dark, spongy or powdery deposits over normal plating current densities necessitating addition of complexing agents or organic additives. The properties of the coatings are strongly related to the morphological and structural characteristics of the deposits that depend on the operating conditions, nature of additive added, mode of current applied, etc.

Pulse electrodeposition has been found to be a powerful means for controlling the electrocrystallization process and hence producing deposits with unique structures and properties. In pulse plating, three different parameters namely, ON-time ($T_{ON}$), OFF-time ($T_{OFF}$), and pulse peak current density ($j_P$) can be varied independently unlike direct current (DC) electrodeposition where the only variable is current density [7].

Nanocrystalline zinc deposits were obtained at relatively higher peak current density by employing pulse current [8–10]. With the aid of additives [8–12], the authors could produce zinc deposits with a grain size of 56 nm with remarkable increase in hardness [8]. Vasilakopoulos et al. [13] reported that pulse technique results in leveling off the DC growth-dependent habits and established that a [00.2] texture at 20 $Adm^{-2}$ resulted in compact zinc deposit.

The present work deals with the influence of the pulse parameters and organic additives on the surface morphology and crystallographic texture of electrodeposited zinc obtained from alkaline non-cyanide bath. The results are compared with DC plating [14].

M. S. Chandrasekar
Indian Institute of Technology, Madras, Chennai 600 036, India

S. Srinivasan
Central ElectroChemical Research Institute, Karaikudi 630006, TN, India

M. Pushpavanam (✉)
Alagappa Chettiar College of Engineering & Technology, Karaikudi 630044, TN, India
e-mail: malathypush@yahoo.com

## Experimental

### Electrolyte and electrolytic cell

The composition of the electrolyte used in this study includes: zinc oxide 9–12 gL$^{-1}$; NaOH 90–120 gL$^{-1}$; pH 13–14 [14]. The prepared bath was given due pretreatments to remove the metallic and organic impurities [15, 16]. Poly vinyl alcohol (primary additive) of 1–2 gL$^{-1}$ and piperonal (secondary additive) of 0.5–1.5 gL$^{-1}$ were prepared as given elsewhere [14].

Pulse electrodeposition was carried out in a 175 mL capacity cell. Mild steel plates were used as the cathode with an exposed area of $2 \times 2$ cm$^2$ to obtain 5-μm thick zinc deposit and (99.99% pure, Aldrich) zinc sheet as a soluble anode. Before electrodeposition, the steel plates were cleaned with trichloroethylene and given cathodic and anodic cleaning for 120 and 30 s, respectively in the conventional alkaline (cleaner) solution. All chemicals used were of Laboratory Grade, supplied by Merck or Fischer.

All electrodeposition experiments were carried out at temperature of 30–35°C. The cathode current efficiency (CCE%) was calculated from the mass gain obtained after deposition.

### Pulse electrodeposition

A DC-regulated pulse power rectifier (Saral Systems, model: PR 1010 TPS, India) was used to generate the pulse waveforms. The effect of each pulse parameters on the deposit quality and properties were studied maintaining the other two constant. The range of pulse variables and additives investigated in this study are: $T_{ON}$ 6–18 ms; $T_{OFF}$ 6–60.7 ms; $j_P$ 2–7 Adm$^{-2}$, and duty cycle ($\gamma$) 9.0–50%.

### Characterization of zinc deposits

A Scanning Electron Microscope (SEM) (Hitachi, model: S3000H, Canada) and Atomic Force Microscope (AFM) (Molecular Imaging Scanning probe microscope, model: PICOSPM, US) were used to characterize the surface morphology and topography of zinc deposits. The grain size of zinc platelet was calculated by averaging the length, width and thickness of each platelet observed and the root-mean-square roughness ($R_{RMS}$) values were determined on the basis of AFM studies.

X-ray diffraction measurements were performed with X'PERT PRO PANalytical, Netherlands (model: PW3040 160) equipped with Cu K$_\alpha$ radiation. Crystallite size was estimated by Scherrer's equation [17] using high intensity reflection of either basal [00.2] or pyramidal [10.1] peaks. The X-ray scan rate was 0.4°/s ranging from 30° to 80°. For accurate measurements of preferred orientations, area under each peak of the XRD patterns was determined. Relative texture coefficient (RTC in %) for the reflections [hk.l] were calculated by the formula [18]:

$$\text{RTC }(hk.l) = \frac{(\text{TC}_{hk.l})_E}{(\text{TC}_{hk.l})_S} \times 100 \text{ and}$$

$$\text{TC }(hk.l) = \frac{(R_{hk.l})_E}{(R_{hk.l})_S} \times 100$$

where TC, texture co-efficient of the planes ($hk.l$); $R_{hkl}$, area under reflection intensity corresponding to [$hk.l$] plane; E, sample under study; S, reagent grade zinc powder sample (of <325 mesh) to serve as a reference for the zinc samples.

## Results and discussion

The nucleation rate is enhanced and the grain size of deposit is usually decreased because of higher $j_P$, however, the effect of $T_{ON}$ and $T_{OFF}$ on deposit characteristics cannot be predicted for certain systems, because the crystallization process is strongly influenced by adsorption and desorption phenomena. Therefore, each system may react differently during the electro-crystallization process yielding different surface morphology.

### Effect of OFF-time on the surface morphology and crystallographic orientation

Figure 1 shows that crystallite size decreases till 51.5 ms ($T_{OFF}$) and increases at 60.7 ms. The influence of $T_{OFF}$ on the grain size and morphology of zinc deposits is shown in Fig. 2. The average grain size of zinc deposits decreased gradually with increasing $T_{OFF}$. A similar trend has been reported for electrodeposition of cadmium from acid bath [19]. This has been attributed to the adsorption of an inhibiting species probably the hydroxyl anions, which blocks the growth centers of the cathode and enhance new nuclei at each pulse. Therefore, longer the $T_{OFF}$ finer would be the grains [20].

Figure 2a shows that at lower $T_{OFF}$, the deposit surface consisted of uniform well-facetted crystallites. However, increase in $T_{OFF}$ resulted in a progressive decrease in number of the pyramidal and prismatic shaped crystals accompanied with decrease in average grain size of "background" grains (Fig. 2b, c). Bright and smooth deposit was obtained at 51.5 ms ($T_{OFF}$) at constant 6 ms ($T_{ON}$) and 2 Adm$^{-2}$ ($j_P$) and hence, this condition was optimized for rest of the experiments.

Figure 3 shows the influence of $T_{OFF}$ on the crystallographic orientation of the zinc deposits. SEM images are in agreement with XRD that showed very sharp peaks
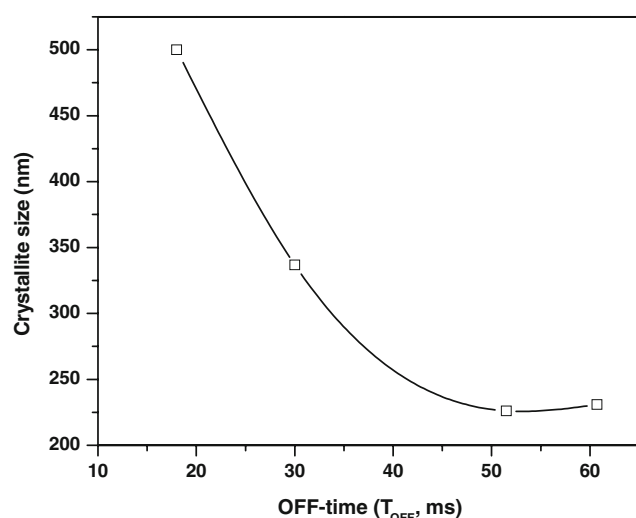
**Fig. 1** Variations of crystallite size (nm) of zinc deposits produced from additives free electrolyte at constant $T_{ON} = 6$ ms, $j_P = 2$ Adm$^{-2}$ and at different $T_{OFF}$

characteristic of micrograins (Fig. 3a). Percentage orientations of basal [00.2] plane increases while RTC of prismatic [10.0] plane decreases with increase in $T_{OFF}$ (Fig. 3b). Pyramidal planes [10.1], [10.2] and [10.3] show erratic percentage orientations with $T_{OFF}$. At 18 ms ($T_{OFF}$), 29.07% of the zinc crystallites oriented to basal [00.2], 22.03% to [10.2] and 23.57% to [10.3] planes. With increase in $T_{OFF}$ to 60.7 ms, only 4.4% of crystallites were

oriented to prismatic plane while majority of crystallites preferred to form basal [00.2] and another pyramidal [10.3] planes which corresponds to low overpotential [21–23].

### Effect of ON-time on the surface morphology and crystallographic orientation

Figure 4 shows that crystallite size increases with the increase in $T_{ON}$ in the range 226–416 nm. At 6 ms ($T_{ON}$) (Fig. 2c), the deposit surface shows average finer grains with well-facetted crystallites. This effect is due to an enhancement of the nucleation rate [24]. According to pulse plating theory [25], the thickness of the pulsating part of diffusion layer is a function of $T_{ON}$. If the latter's thickness is small compared to the surface roughness of the base metal, which is possible at sufficiently short $T_{ON}$, compact deposits are formed. Figure 5a shows that for 9 ms ($T_{ON}$), the surface morphology of the deposit consists of large and well-facetted pyramidal shaped crystallites [26] surrounded by uniform finer grains. Increasing the $T_{ON}$, which in turn increased duty cycle led to a decrease in size of the large pyramidal shaped crystallites and ultimately, to their complete disappearance and uniform replacement with the large and finer grains at 18 ms ($T_{ON}$) as shown in Fig. 5b. A similar behavior was reported during pulse electrodeposition of zinc from a chloride bath [8]. It was argued that the thickness of the pulsating diffusion layer at the longest $T_{ON}$ used in that study (7 ms) was close to that of the steady-state diffusion layer.

**Fig. 2** SEM images of the surface morphology of zinc deposits produced from additives free electrolyte at constant $T_{ON} = 6$ ms, $j_P = 2$ Adm$^{-2}$ and different OFF-time ($T_{OFF}$) of **a** 18 ms, **b** 30 ms, **c** 51.5 ms
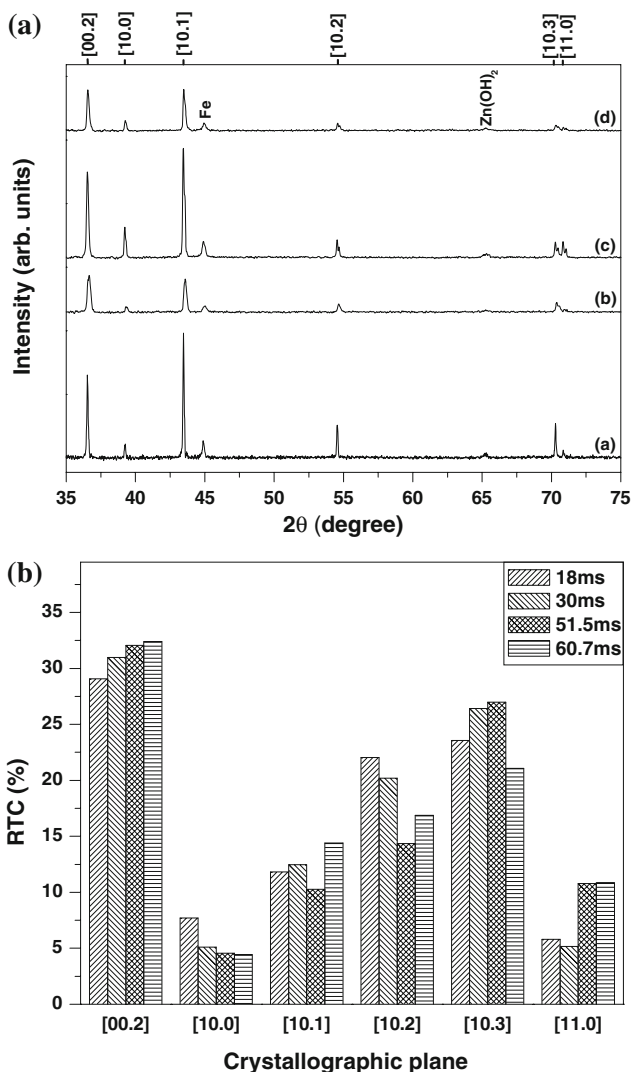
**(a)**



**(b)**
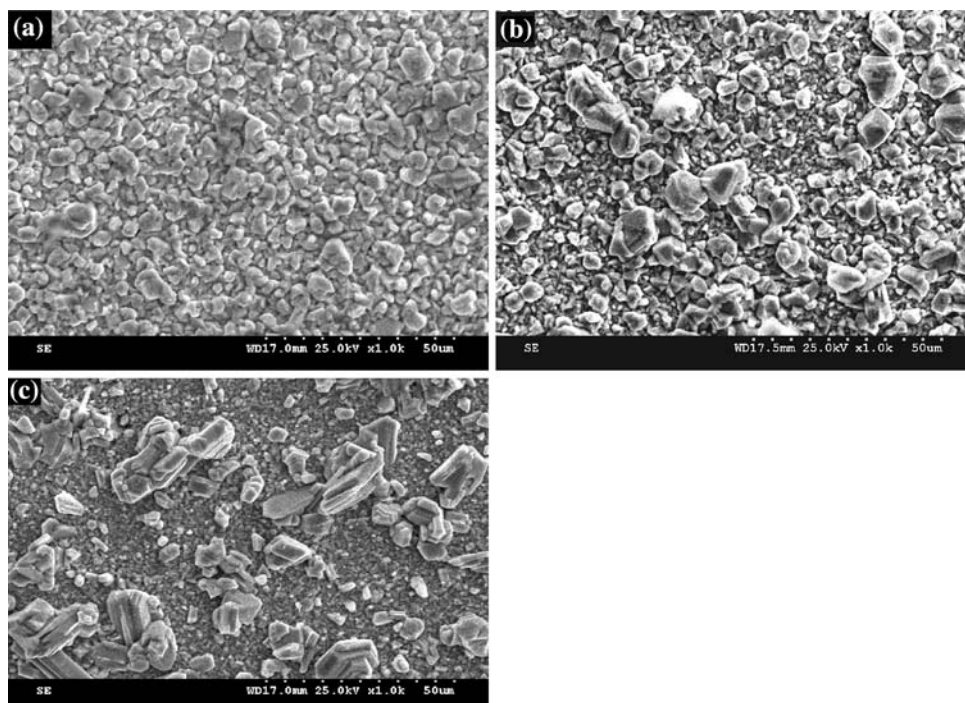


Fig. 3 **a** XRD patterns of zinc deposits produced from additives free electrolyte at constant $T_{ON} = 6$ ms, $j_P = 2$ Adm$^{-2}$ and various OFF-time ($T_{OFF}$) of (*a*) 18 ms, (*b*) 30 ms, (*c*) 51.5 ms, (*d*) 60.7 ms. **b** Schematic representations of percentage RTC as a function of crystallographic planes of zinc deposits produced from additives free electrolyte at $T_{ON} = 6$ ms, $j_P = 2$ Adm$^{-2}$, and various $T_{OFF}$

Therefore, at large duty cycle pulse current resembled DC electrolysis that contributes to a large-grained structure [8].

The crystallographic orientation of zinc deposits obtained with increasing $T_{ON}$ is shown in Fig. 6. The sharp peaks confirm the microcrystalline morphology (Fig. 6a). At 6 ms ($T_{ON}$), the zinc deposits consists of 29.06% of grains oriented to basal [00.2], 7.71% to prismatic [10.0], 11.82% to [10.1], 22.03% to [10.2], 23.57% to [10.3], and rest to [11.0] planes (Fig. 6b). Increase in $T_{ON}$ to 18 ms results in 27.36 and 20.47% of crystallites were oriented to [00.2] and [10.3] planes, respectively, while 33.52% of zinc crystallites oriented to prismatic [10.0] which correspond to high overpotential [21].
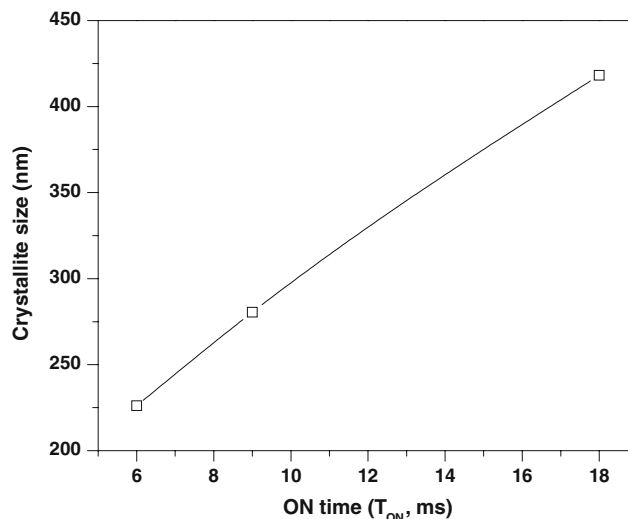


Fig. 4 Variations of crystallite size (nm) of zinc deposits produced from additives free electrolyte at constant $T_{OFF} = 51.5$ ms, $j_P = 2$ Adm$^{-2}$ and at different $T_{ON}$

### Effect of pulse peak current density on the surface morphology and crystallographic orientation in presence of additives

Addition of organic additives during electrodeposition could easily segregate grain boundaries and weaken the coating properties [27, 28]. As discussed above, good and smooth zinc deposits were obtained at 51.5 ms ($T_{OFF}$) and 6 ms ($T_{ON}$). Hence at these optimized $T_{OFF}$ and $T_{ON}$ values, the effect of $j_P$ was studied with additives and additive-free electrolytes, independently.

### *Effect of pulse peak current density on the surface morphology and crystallographic orientation in absence of additives*

Figure 7 shows SEM images of zinc deposits obtained in absence of additives at different $j_P$ values. Comparing Fig. 2c (at 2 Adm$^{-2}$) and Fig. 7, it is clear that increasing $j_P$ to 5 Adm$^{-2}$ (Fig. 7a) results in a progressive decrease in grain size. The smallest crystallite size of about 210 nm was obtained at 5 Adm$^{-2}$. In Fig. 7b, grains with a laminated texture were observed. Even at 7 Adm$^{-2}$, with pulse technique, it was difficult to prepare nanocrystalline (grain size <100 nm) zinc from additive-free electrolyte. SEM studies show that increasing $j_P$ from 2 to 5 Adm$^{-2}$ leads to a progressive reduction in grain size may be due to increase in overpotential as reported in literature [7–9, 19, 20, 23].

The crystallographic orientation of zinc deposits obtained with increasing $j_P$ is shown in Fig. 8. Increasing the $j_P$ results in change of orientation from basal [00.2] plane formed at 2 Adm$^{-2}$ to pyramidal plane [10.2] at 5

Fig. 5 SEM images of the
surface morphology of zinc
deposits produced from
additives free electrolyte at
constant $T_{OFF} = 51.5$ ms,
$j_P = 2$ Adm$^{-2}$ and different
ON-time ($T_{ON}$) of a 9 ms,
b 18 ms
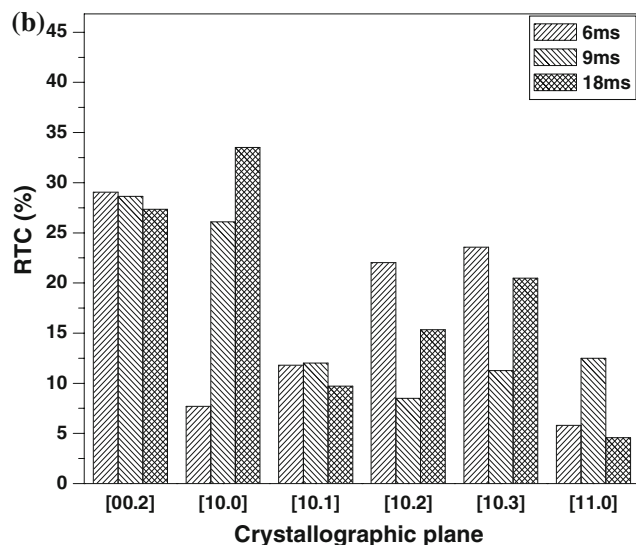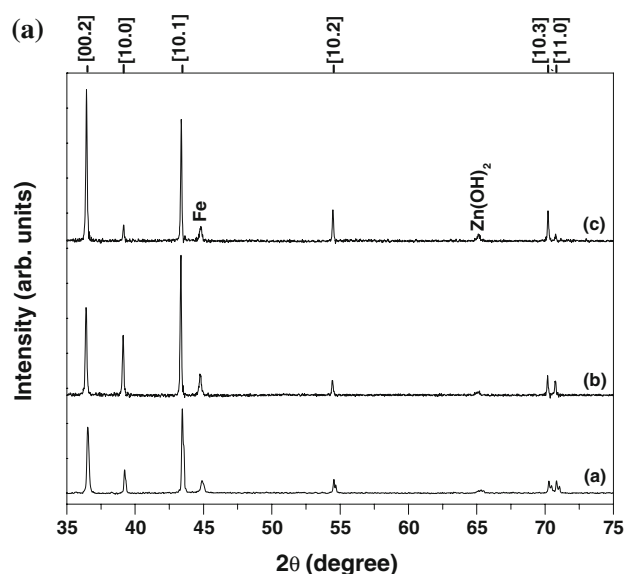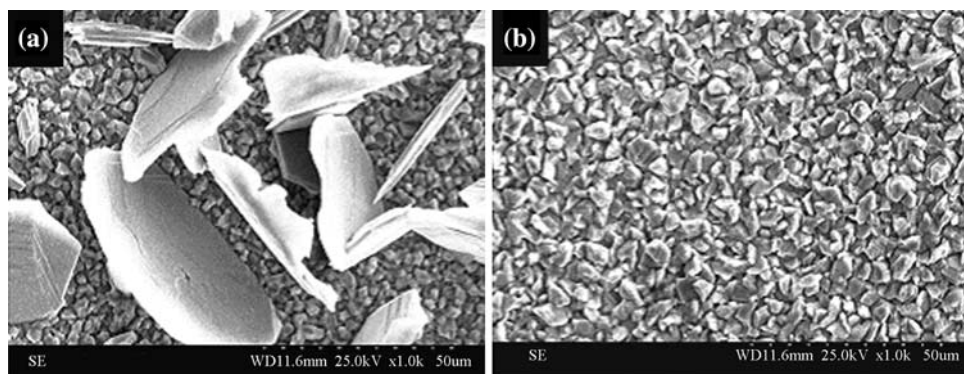




Fig. 6 a XRD patterns of zinc deposits produced from additives free
electrolyte at constant $T_{OFF} = 51.5$ ms, $j_P = 2$ Adm$^{-2}$ and various
ON-time ($T_{ON}$) of (a) 6 ms, (b) 9 ms, (c) 18 ms. b Schematic
representations of percentage RTC as a function of crystallographic
planes of zinc deposits produced from additives free electrolyte at
$T_{OFF} = 51.5$ ms, $j_P = 2$Adm$^{-2}$, and various $T_{ON}$ (without additives)

Adm$^{-2}$. At 5 Adm$^{-2}$, 40% of zinc crystallites are oriented
to [10.2], 23.5% to [10.3], 15.5% to [11.0], 14.1% to
[10.1], and 4.7% to [00.2] while rest to prismatic [10.0]
planes (Table 1). At higher $I_P$, pyramidal planes [10.2] and
[10.3] dominant with each 28.2%.

### Effect of addition of PVA on the surface morphology and crystallographic orientation

Figure 9a–c shows the morphology of zinc deposits
obtained at various PVA concentrations at 5 Adm$^{-2}$. At 1.0
gL$^{-1}$ PVA, deposit consists of layered structure as com-
pared to coarse grains (Fig. 7a) obtained without additive.
Adherent and compact deposit is obtained at 1.5 gL$^{-1}$ PVA
(Fig. 9b) as compared to deposit (Fig. 9c) obtained with
2.0 gL$^{-1}$ PVA. Comparison of Fig. 7 with Fig. 9 shows the
disappearance of the sharp edges of the pyramidal grains
accompanied with a slight reduction in the grain size. Some
studies on DC-plated zinc [14], pulse-plated nickel [20,
29–31], and zinc [7, 8] with organic additives show a
similar trend.

The grain size of zinc deposits at 5 Adm$^{-2}$ decreased
with increasing PVA concentration above 1.5 gL$^{-1}$ but at
the expense of deposit's quality (Fig. 9c, d). Therefore, the
optimized 1.5 gL$^{-1}$ PVA concentration is used for the rest
of the present study [14], which gives the smallest grain
size of 200 nm at 5 Adm$^{-2}$. The ability of PVA to refine
the grain size may be due to (i) increasing the high over-
potential and (ii) retardation of growth and increase in the
effective nucleation rate [23].

The crystallographic orientation of zinc deposits
obtained with various $j_P$ (5 and 7 Adm$^{-2}$) and PVA con-
centration is shown in Fig. 10. The percentage of planes
[00.2], [10.0], [10.1], [10.2], [10.3], and [11.0] varies with
PVA concentration and $j_P$. Zinc deposit produced from
electrolyte containing 1.5 gL$^{-1}$ PVA at 5 Adm$^{-2}$ con-
tained 54.9 and 25.6% of zinc crystallites oriented parallel
to prismatic [10.0] and pyramidal [10.1] plane, respec-
tively, while at 7 Adm$^{-2}$, 27.2 and 45% of crystallites were
oriented towards [10.2] and [10.3] planes, respectively,

**Fig. 7** SEM images of the surface morphology of zinc deposits produced from additives free electrolyte at constant $T_{OFF} = 51.5$ ms, $T_{ON} = 6$ ms and different pulse peak current density ($j_P$) of **a** 5 Adm$^{-2}$, **b** 7 Adm$^{-2}$





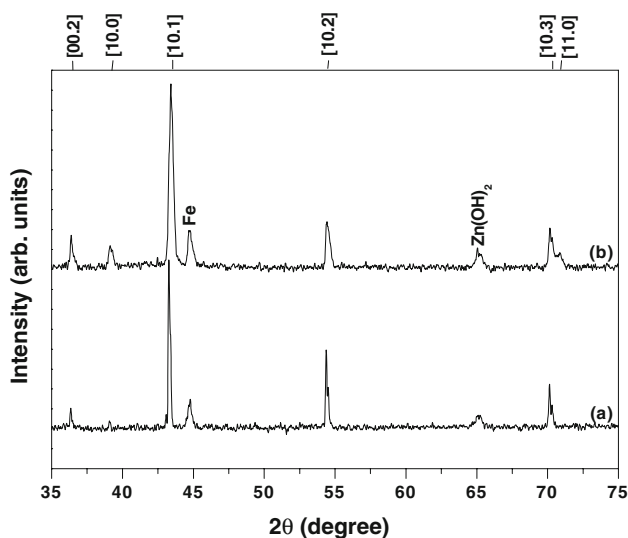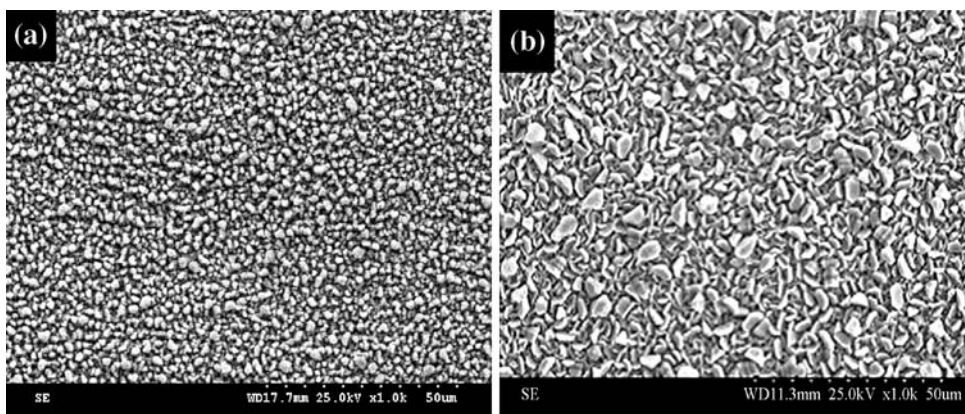**Fig. 8** XRD patterns of zinc deposits produced from additives free electrolyte at constant $T_{OFF} = 51.5$ ms, $T_{ON} = 6$ ms and various peak current density ($j_P$) of **a** 5 Adm$^{-2}$, **b** 7 Adm$^{-2}$

(Table 1). The presence of PVA showed a pseudo-texture since its addition affects the electrocrystallization process with a consequence to alter the texture of the deposits [27].

### Effect of piperonal in presence of PVA on the surface morphology and crystallographic orientation

The surface morphologies of deposits produced at various PIP concentrations at 5 Adm$^{-2}$ are shown in Fig. 11a–c. Deposits produced from PIP-free electrolyte with 1.5 gL$^{-1}$ PVA show a prismatic shaped morphology (Fig. 9). The average grain size of the platelets decreased with the addition of PIP. Fine-grained deposit with an average crystallite size of 34 nm is obtained at 1.0 gL$^{-1}$ PIP and 5 Adm$^{-2}$. The improvement in quality of the deposit along with grain refinement at 1.0 gL$^{-1}$ PIP was attributed to the higher cathodic overpotential [8]. However, increase in PIP content to 1.5 gL$^{-1}$ at 5Adm$^{-2}$ (Fig. 11c) and also increase in $j_P$ to 7 Adm$^{-2}$ at 1.0 gL$^{-1}$ PIP (Fig. 11d) produced poor quality deposits. Hence, the crystallite size decreases with addition of additives than without additives may be due to increased (1) nucleation rate and (2) overpotential and lower surface ad-atoms concentration [7].

The crystallographic orientation of zinc deposits obtained with various $j_P$ (5 and 7 Adm$^{-2}$) and PIP concentration is shown in Fig. 12. From Table 1, in presence of PVA and PIP, 68.5% and 72.3% of crystallites are orientated parallel to the prismatic [10.0] planes at 5 and

**Table 1** Relative texture coefficient (RTC in %) of pulse-plated zinc

| [hk.l] | Without additives | | | With 1.5 gL$^{-1}$ PVA | | With 1.5 gL$^{-1}$ PVA + 1.0 gL$^{-1}$ PIP | |
|---|---|---|---|---|---|---|---|
| | 2 Adm$^{-2}$ | 5 Adm$^{-2}$ | 7 Adm$^{-2}$ | 5 Adm$^{-2}$ | 7 Adm$^{-2}$ | 5 Adm$^{-2}$ | 7 Adm$^{-2}$ |
| [00.2] | 32.1 | 4.7 | 7.7 | 5.5 | 7.6 | 8.4 | 8.6 |
| [10.0] | 4. 6 | 2.1 | 10.4 | 54.9 | 5.7 | 68.5 | 72.3 |
| [10.1] | 10.3 | 14.1 | 17.8 | 25.6 | 5.6 | 9.8 | 7.5 |
| [10.2] | 14.4 | 40.0 | 28.2 | 5.1 | 27.2 | 3.5 | 2.1 |
| [10.3] | 27.0 | 23.5 | 28.2 | 3.6 | 45.0 | 2.5 | 1.4 |
| [11.0] | 10.8 | 15.5 | 7.7 | 5.3 | 8.9 | 7.3 | 8.0 |

**Fig. 9** SEM images of the surface morphology of zinc deposits obtained at constant $T_{OFF} = 51.5$ ms, $T_{ON} = 6$ ms, $j_P = 5$ Adm$^{-2}$ and at various PVA additive concentration (gL$^{-1}$) **a** 1.0, **b** 1.5, **c** 2.0, **d** 1.5 gL$^{-1}$ PVA at $j_P = 7$ Adm$^{-2}$
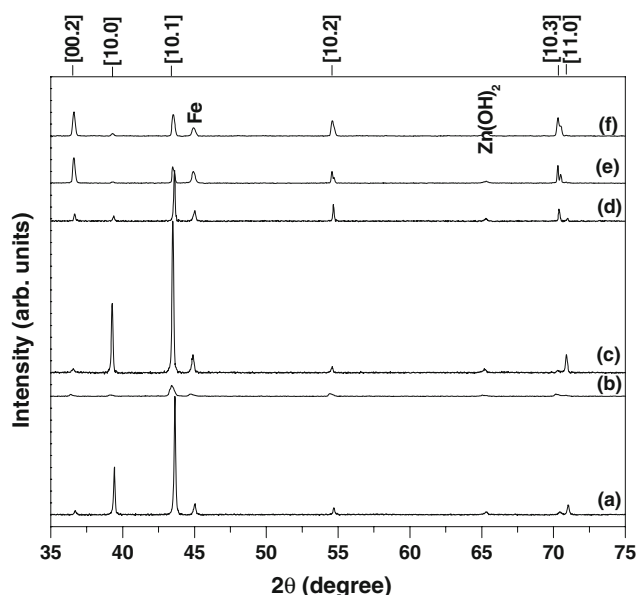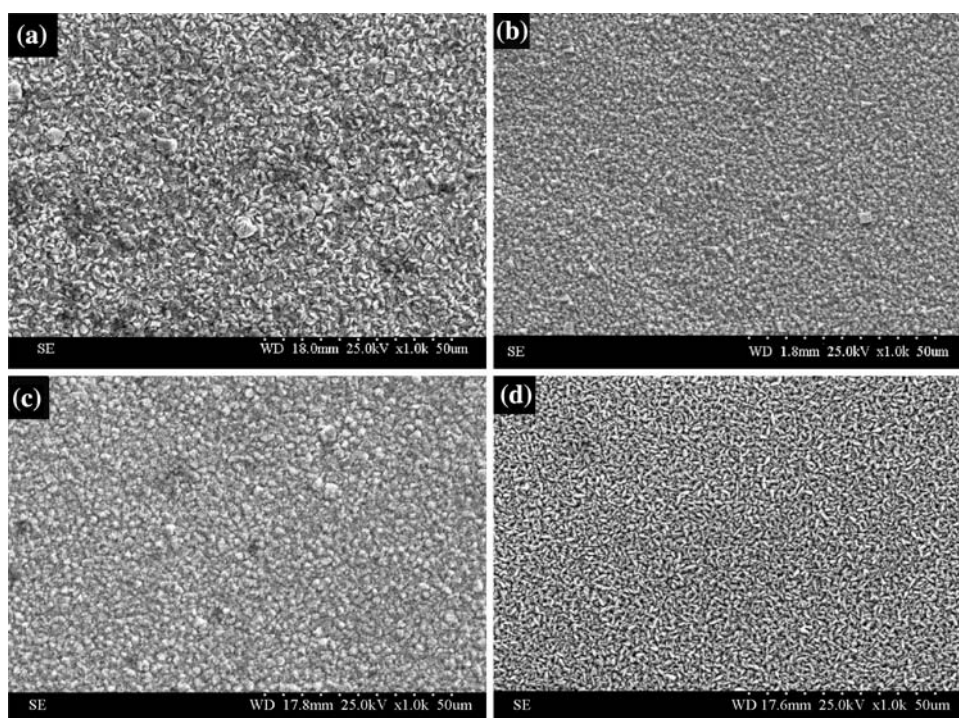




**Fig. 10** XRD patterns of zinc deposits at constant $T_{OFF} = 51.5$ ms, $T_{ON} = 6$ ms and various $j_P$ and PVA concentration: (*a*) 1.0 gL$^{-1}$ PVA at 5 Adm$^{-2}$, (*b*) 1.5 gL$^{-1}$ PVA at 5 Adm$^{-2}$, (*c*) 2.0 gL$^{-1}$ PVA at 5 Adm$^{-2}$, (*d*) 1.0 gL$^{-1}$ PVA at 7 Adm$^{-2}$, (*e*) 1.5 gL$^{-1}$ PVA at 7 Adm$^{-2}$, and (*f*) 2.0 gL$^{-1}$ PVA at 7 Adm$^{-2}$

7 Adm$^{-2}$, respectively. This indicates that in the presence of additives, [10.0] is the preferred crystallographic orientation. This might be due to the fact that additives adsorbs onto the growing deposit. This affects the electrocrystallization process with a consequence to alter the texture of the deposits [16].

Figure 13 shows the effect of $j_P$ on CCE. CCE increases with increase in $j_P$ both with and without additives. Deposits obtained with 1.5 gL$^{-1}$ PVA shows high current efficiency (95.2%) compared to those obtained in presence of 1.5 gL$^{-1}$ PVA + PIP (90%) and without additives (88.34%) at 5 Adm$^{-2}$. This confirms that the additives increase overpotential due to specific adsorption. The result is in agreement with literature data [14, 23]. As discussed in Ref. [14], zinc deposit from zincate electrolyte without additives could yield only powdery, non-adherent deposits. This is due to the faster rate of reduction of zinc ions than the rate of transport of electro-active species in the solution. Though this is improved under pulse conditions, an additive is essential to complex the zinc ions and to control the rate determining step. PVA does this job by forming a complex with zinc ions yielding adherent deposits. Deposition from a complex solution always results in higher overpotential. However, the change from loose deposition (difficult to precisely estimate the mass of deposition) to compact deposition enables increase in CCE. However, to obtain bright deposits, another brightener (PIP) is essential. This, by specific adsorption on the substrate refines grain size further to produce bright coatings, however, the increase in overpotential caused by specific adsorption, causes moderate reduction in deposition efficiency.

**Fig. 11** SEM images of the surface morphology of zinc deposits obtained at constant $T_{OFF} = 51.5$ ms, $T_{ON} = 6$ ms, $j_P = 5$ Adm$^{-2}$, 1.5 gL$^{-1}$ PVA and at various PIP concentration (gL$^{-1}$) **a** 0.5, **b** 1.0, **c** 1.5, **d** 1.0 gL$^{-1}$ PIP at $j_P = 7$ Adm$^{-2}$
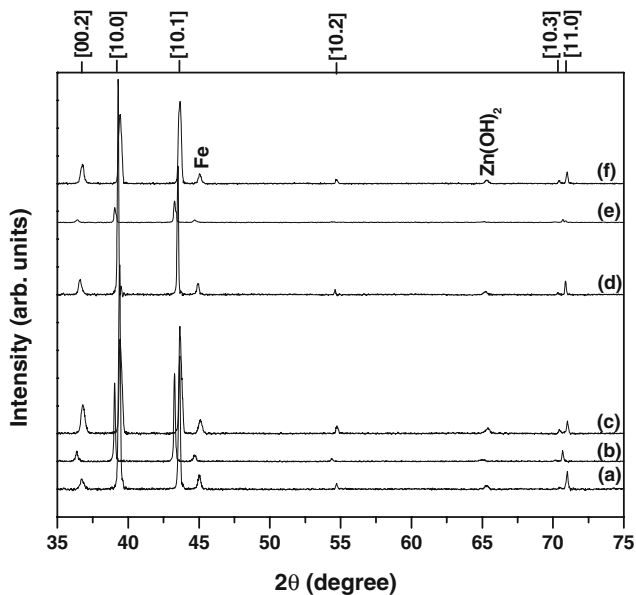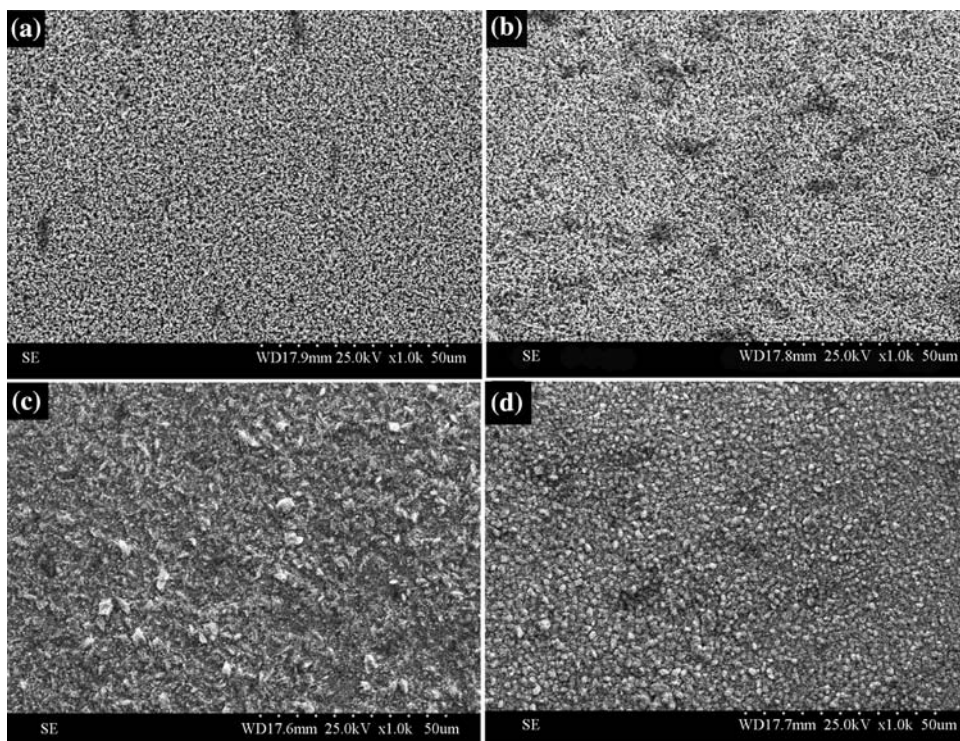


**Fig. 12** XRD patterns of zinc deposits at $T_{OFF} = 51.5$ ms, $T_{ON} = 6$ ms, PVA = 1.5 gL$^{-1}$ and at various $j_P$ and PIP concentration: (a) 0.5 gL$^{-1}$ PIP at 5 Adm$^{-2}$, (b) 1.0 gL$^{-1}$ PIP at 5 Adm$^{-2}$, (c) 1.5 gL$^{-1}$ PIP at 5 Adm$^{-2}$, (d) 0.5 gL$^{-1}$ PIP at 7 Adm$^{-2}$, (e) 1.0 gL$^{-1}$ PIP at 7 Adm$^{-2}$, and (f) 1.5 gL$^{-1}$ PIP at 7 Adm$^{-2}$
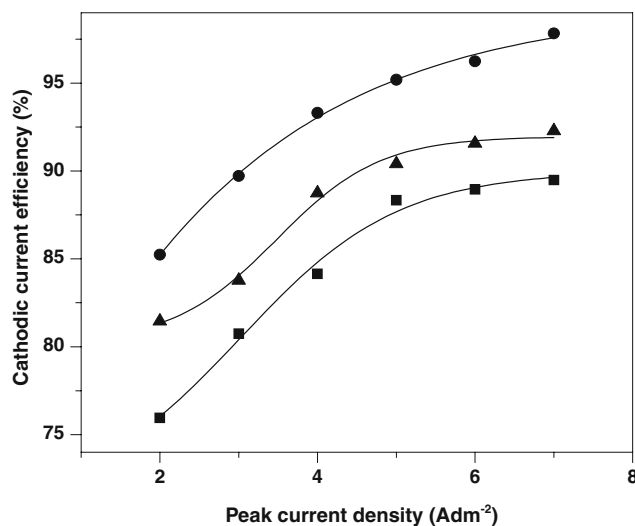


**Fig. 13** Variations of CCE of zinc deposits with pulse current densities ($j_P$) at constant $T_{OFF} = 51.5$ ms and $T_{ON} = 6$ ms: *square* without additive, *circle* 1.5 gL$^{-1}$ PVA, and *triangle* 1.5 gL$^{-1}$ PVA + 1.0 gL$^{-1}$ PIP

## Topography and grain size

AFM images, representing the influence of $j_P$ with additive concentrations (1.5 gL$^{-1}$ PVA and 1.0 gL$^{-1}$ PIP) on the surface structure of zinc coatings are presented in Fig. 14.

Surface topography investigations on the μm level (5 × 5 μm scanned surface area) have shown that DC-plated coatings consisted of number of nanocrystallite grains as shown in Fig. 14a, b. The values of the grain size of DC deposited coatings varied between 80 and 160 nm, with the average of 87 nm. The average surface roughness ($R_{RMS}$) of DC-plated zinc coating was 135 nm.
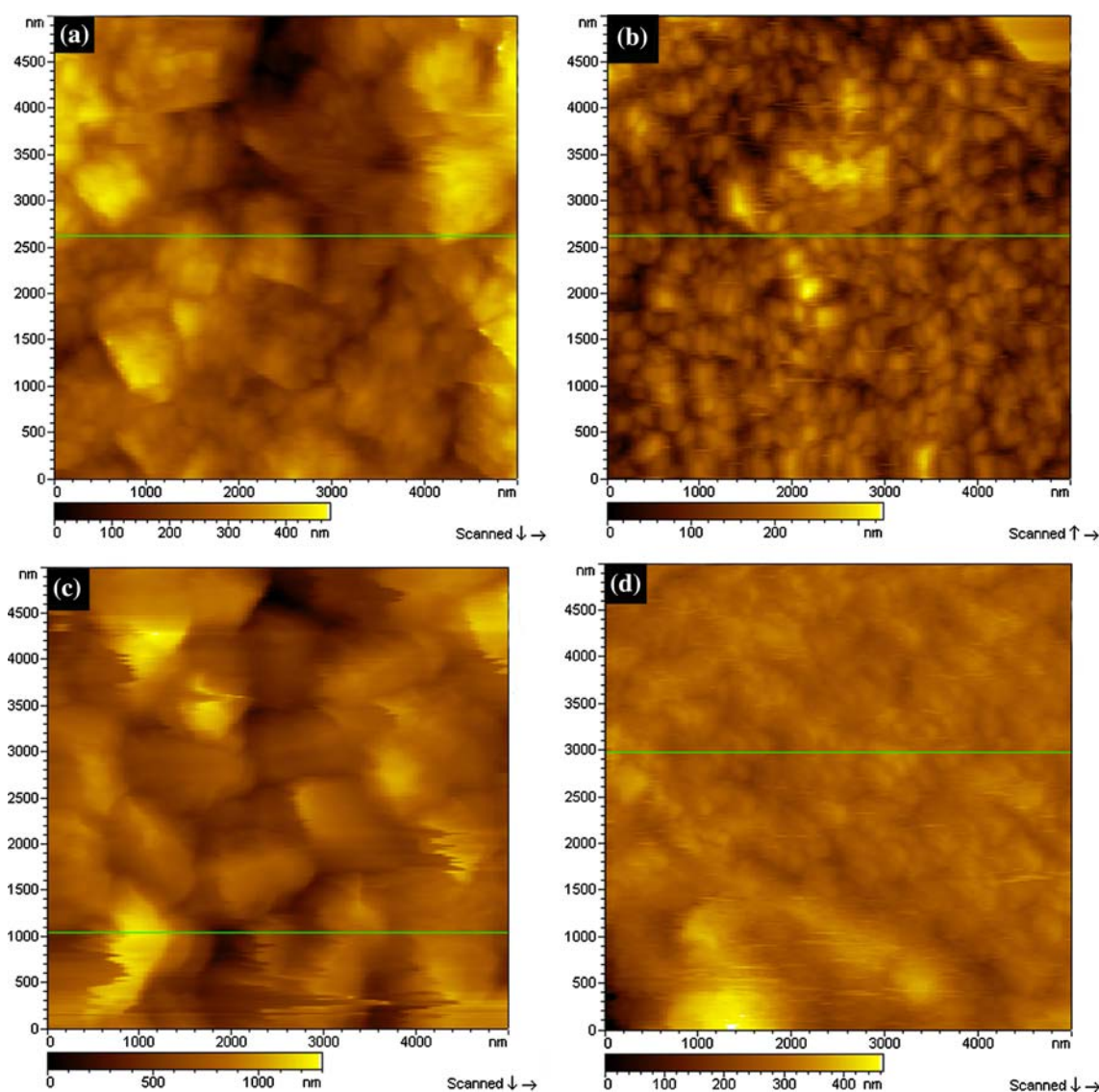
**Fig. 14** AFM images of zinc coatings obtained by DC at 2 Adm$^{-2}$ containing **a** 1.5 gL$^{-1}$ PVA, **b** 1.5 gL$^{-1}$ PVA + 1.0 gL$^{-1}$ PIP and by PC at 6 ms ($T_{ON}$), 51.5 ms ($T_{OFF}$), 5 Adm$^{-2}$ ($j_P$) containing **c** 1.5 gL$^{-1}$ PVA, **d** 1.5 gL$^{-1}$ PVA + 1.0 gL$^{-1}$ PIP. The scanned area 5 × 5 μm$^2$

The main difference in the morphology of electrodeposits obtained by the DC and pulse techniques is in the crystallite size. Pulse-plated coatings were more compact and possessed a more homogeneous structure (i.e., more uniform agglomeration size). Besides, these coatings were significantly smoother as their $R_{RMS}$ numbers varied between 30 and 75 nm (Fig. 14c, d) and are lower than that of DC-plated sample (135 nm).

An increase in cathodic current in the pulse plating of metals usually causes a decrease in the grain size only in a certain $j_P$ range applied. The increase in $j_P$ from 2, 4, 5, and 7 Adm$^{-2}$ caused reduction in the average grain size. However, further increase in $j_P$ (>7Adm$^{-2}$) resulted in dark deposit with discrete large crystallites. The smoothest surface of zinc deposits with $R_{RMS}$ of 44 nm was obtained

at $T_{OFF}$ 51.5 ms; $T_{ON}$ 6 ms; $j_P$ 5 Adm$^{-2}$; PVA 1.5 gL$^{-1}$, and PIP 0.5 gL$^{-1}$ (Fig. 14d).

## Conclusion

Adherent and bright nanocrystalline zinc deposits with preferred orientation of plane [10.0] and average crystallite size of 34 nm was produced from an alkaline non-cyanide electrolyte with additives. Increasing $T_{ON}$ in the range of 6–18 ms resulted in increased grain size. Increasing the $T_{OFF}$ in the range of 6–60.7 ms was found to yield fine grained deposits. Grain refinement was also observed by increasing $j_P$ up to 5 Adm$^{-2}$. Zinc deposits produced from electrolyte without additives showed random orientations

while deposits produced from bath containing additives showed preferred orientations. The advantages of pulse electrodeposition from this study include (1) an agent for effective grain refinement, at moderate current densities of deposition, enabling the preparation of compact deposits and (2) 50% less additive concentration is sufficient to obtain high quality deposit [16] as compared to DC [14]. The new bath also has the additional advantage of being eco-friendly in that it uses only easily disposable organics.

# References

1. Krzywicki JW (2006) Metal Finish 104:28
2. Chandrasekar MS, Shanmugasigamani S, Pushpavanam M (2009) J Solid State Electrochem 13:781
3. Ramanauskas R, Juškenas R, Kalinicenko A, Garfias-Mesias LF (2004) J Solid State Electrochem 8:416
4. Ramanauskas R, Gudaviciute L, Kalinicenko A, Juškenas R (2005) J Solid State Electrochem 9:900
5. Pech-Canul MA, Ramanauskas R, Maldonado L (1997) Electrochim Acta 42:255
6. Ramanauskas R, Gudaviciute L, Juskenas R, Scit O (2007) Electrochim Acta 53:1801
7. Chandrasekar MS, Pushpavanam M (2008) Electrochim Acta 53:3313
8. Kh Saber, Koch CC, Fedkiw PS (2003) Mater Sci Eng A 341:174
9. Youssef KhMS, Koch CC, Fedkiw PS (2004) J Electrochem Soc 151:C103
10. Li MC, Jiang LL, Zhang WQ, Qian YH, Luo SZ, Shen JN (2007) J Solid State Electrochem 11:549
11. Li MC, Jiang LL, Zhang WQ, Qian YH, Luo SZ, Shen JN (2007) J Solid State Electrochem 11:1319
12. Youssef KhMS, Koch CC, Fedkiw PS (2004) Corrosion Sci 46:51
13. Vasilakopoulos D, Bouroushian M, Spyrellis N (2006) J Mater Sci 41:2869. doi:10.1007/s10853-005-5161-z
14. Shanmugasigamani S, Pushpavanam M (2006) J Appl Electrochem 36:315
15. Geduld H (1988) Zincate or alkaline non-cyanide zinc plaing in "zinc plating". ASM International Metals Park, Ohio, p 90
16. Chandrasekar MS, Shanmugasigamani S, Pushpavanam M (2009) Mater Chem Phys 115:603
17. Cullity BD (1978) Elements of X-ray diffraction, 2nd edn. Addison-Wesley, Philippines
18. Berube LPh, L'Esperance G (1989) J Electrochem Soc 136:2314
19. Puippe JCl, Ibl N (1980) Plat Surf Finish 67:68
20. El-Sherik AM, Erb U, Page J (1996) Surf Coat Technol 88:70
21. Pangarov NA (1965) J Electroanal Chem 9:70
22. Vasilakopoulos D, Bouroushian M, Spyrellis N (2001) Trans Inst Metal Finish 79:107
23. Choo RTC, Toguri JM, El-Sherik AM, Erb U (1995) J Appl Electrochem 25:384
24. Paatsch W (1986) In: Puippe JCl, Leaman F (eds) Theory and practice of pulse plating. AESF Publication, Orlando, Florida, p 93
25. Ibl N (1979) Metalloberflache 33:51
26. Fischer H (1972–1973) Electrodeposition Surf Treatment 1:319
27. Mouanga M, Ricqa L, Berco P (2008) Surf Coat Technol 202:1645
28. Koch CC (2007) J Mater Sci 42:1403. doi:10.1007/s10853-006-0609-3
29. Kim Sh, Aust KT, Erb U, Gonzalez F, Palumbo G (2003) Scripta Mater 48:1379
30. Mishra AC, Thakur AK, Srinivas V (2009) J Mater Sci 44:3520. doi:10.1007/s10853-009-3475-y
31. El-Sherik AM, Erb U (1995) J Mater Sci 30:5743. doi:10.1007/BF00356715